Survey instruments.
Elaborate thermometers for *in vivo* or *in vitro* studies.
A look at microwave telephony, microwave diathermy, and hyperthermia.
Environmental rf levels around radio and TV transmission towers.
The microwave auditory phenomenon.
Electric and magnetic fields near extra high-voltage transmission lines.
Possible bioeffects due to induced currents or microshocks.
Instrumentation for measuring 60-Hz ac fields.
Leakage currents from household appliances.

Section III: Ultrasound

Physics of ultrasound in inhomogeneous media.
Absorption and reflection.
Acoustic impedance.
Relative absorption due to fat, bone, and muscle.
Piezoelectric transducers.
Ultrasonic ranging devices and images.
Heating or tissue disruptors.
Biophysical mechanisms for sonically generated heat.
Breathing oscillations.
Resonance, cavitation and microstreaming.
Stable versus transient cavitation.
Minimum levels for observed bioeffects.

[1]R. K. Wangsness, *Electromagnetic Fields* (Wiley, New York, 1979).
[2]M. Karplus and R. N. Porter, *Atoms and Molecules* (Benjamin, Menlo Park, CA, 1971).
[3]*Radiofrequency Electromagnetic Fields—Properties, Quantities and Units, Biophysical Interaction, and Measurements* (National Council on Radiation Protection and Measurements Report No. 67) (NCRP, Washington, 1981).
[4]Non-ionizing Radiation (Proceedings of a topical symposium by the American Conference of Governmental Industrial Hygienists, Inc.) (ACGIH, Cincinnati, OH, 1980).
[5]M. L. Walbarsht and D. H. Sliney, Proc. Soc. Photo-Opt. Instrum. Eng. **229** (1980).
[6]D. Sliney and M. Walbarsht, *Safety with Lasers and Other Optical Sources—A Comprehensive Handbook* (Plenum, New York, 1980).
[7]*Biological Effects and Health Hazards of Microwave Radiation*, edited by P. Cyerki (Polish Medical Publishers, Warsaw, 1974).
[8]Complete issue of Proc. IEEE **80** (1) (1980).
[9]A. R. Sheppard and M. Eisenbud, *Biological Effects of Electric and Magnetic Fields of Extremely Low Frequency* (New York University, New York, 1977).
[10]R. A. Tell, Environmental Protection Agency Report No. EPA-520/2-76-008 (1977) (unpublished).
[11]M. Wigder, Environmental Protection Agency Technical Note ORP/EAD 80-1 (1980) (unpublished).
[12]W. Nyborg, Department of Health, Education, and Welfare Report No. HEW-78-8062 (1977) (unpublished).
[13]D. Hazzard, Department of Health, Education, and Welfare Report No. HEW-78-8048 (1978) (unpublished).
[14]Private communication with R. J. Landry at the Bureau of Radiological Health, Rockville, Maryland about ultraviolet hazard monitoring.
[15]Private communication with R. A. Tell at the Environmental Protection Agency, Office of Radiation Programs, Las Vegas, Nevada about microwave rf instrumentation.
[16]R. A. Tell (unpublished), Instrumentation for Measurements of Radiofrequency Electromagnetic Fields: Equipment, Calibration and Selected Applications (prepared for presentation at the course on Advances in Biological Effects and Dosimetry of Low-Energy Electromagnetic Fields held in Sicily, 1981).
[17]E. J. Hall, *Radiology for the Radiologist* (Harper and Row, New York, 1978), pp. 325–348.

Electron impact excitation and uv emission in the Franck–Hertz experiment

Werner Buhr and Werner Klein
I. Physikalisches Institut der Universität zu Köln, 5 Köln 41, Zülpicher Strasse 77, West Germany

S. Pressler
Leybold Heraeus, Köln, 5000 Köln, West Germany

(Received 28 June 1982; accepted for publication 27 October 1982)

With the Franck–Hertz experiment described here the inelastic collision of electrons with mercury atoms and the ultraviolet emission of the excited atoms can be observed simultaneously. The Franck–Hertz tube is a four electrode tube with a concentric system and a quartz window. An electron current stabilization allows the observation of a stepwise increase in light intensity by means of a photomultiplier. The emission spectrum shows the Hg 2536-Å line and two molecular emission bands arising from Hg dimer and trimer transitions. The light emission from the trimer state reveals the influence of geometrical factors of the tube at different accelerating potentials.

I. INTRODUCTION

The description of atoms in terms of energy levels is self-evident today. Thus one tends to underestimate the fundamental importance the experiments of Franck and Hertz assumed historically in understanding the concept of stationary energy states in describing atomic systems.

At the time of their experiments it was uncommon to

characterize the properties of atoms by stationary energy levels. To illuminate this, we cite from the preface of the first edition of Arnold Sommerfeld's *Atombau und Spektrallinien* from 1919:

> Since the discovery of spectral analysis no expert could doubt, that the problem of atoms would be solved if one had learned to understand the language of the spectra.

And later on p. 401:

> The most direct check, most independent from theoretical elements, of Bohr's ideas is given by the method of electron impact. It was founded by Franck and Hertz in 1913... .

In 1914 James Franck and Gustav Hertz[1] reported an experiment on the interaction of electrons with mercury atoms. The authors observed a stepwise loss of electron energy in mercury vapor and, about a month later, were able to show the simultaneous appearance of the mercury resonance line at 2536 Å.[2] In their experiment the ultraviolet emission was detected with a spectrograph using photographic plates. The necessary exposure time varied from one to two hours.

In the years following 1914 many research experiments have been carried out on electron impact excitation.[3] Soon after the advent of quantum mechanics the Franck–Hertz experiment was readily adopted as a fundamental experiment for college and university physics courses. Subsequently many papers on the Franck–Hertz experiment have been published.[4–7] It is probably due to the ease of adopting the experiment to demonstration purposes combined with the advances in the technical development of the Franck–Hertz tube itself that this experiment has become an important asset in almost every experimental lecture on present-day physics. Experimental improvement has been mainly concerned with the automatization or the observation of some additional maxima in the Franck–Hertz curve.

Few modern textbooks call attention to the fact that conclusive evidence for the existence of stationary atomic states is only offered by the simultaneous observation of the consecutive excitations in the current–voltage characteristics and the appearance of the uv-resonance line.

To our knowledge the ultraviolet emission has only been observed once in a demonstration experiment. Füssenich *et al.*[8] report the observation of the 2536-Å line at fixed accelerating voltage of 18, 33, and 40 V employing a modified Franck–Hertz triode tube.[9] It is the purpose of this paper to report for the first time an experiment that allows a simultaneous demonstration of both the current–voltage characteristics and the uv emission.

II. FRANCK–HERTZ TUBE AND EXPERIMENTAL PROCEDURE

The interaction of electrons with atoms is studied in a tube containing an electrode system and mercury vapor. Electrons emitted from a hot cathode are accelerated towards an anode. At certain accelerating voltages the electrons gain enough energy to excite mercury atoms in an inelastic collision. This results in a decrease in anode current. Simultaneously light is emitted as the excited state decays. The excitations occur at accelerating voltages corresponding to integer multiples of the excitation energy.

The essential elements of the Franck–Hertz tube are the electron emitting cathode, a grid to control the emission current, and the anode.

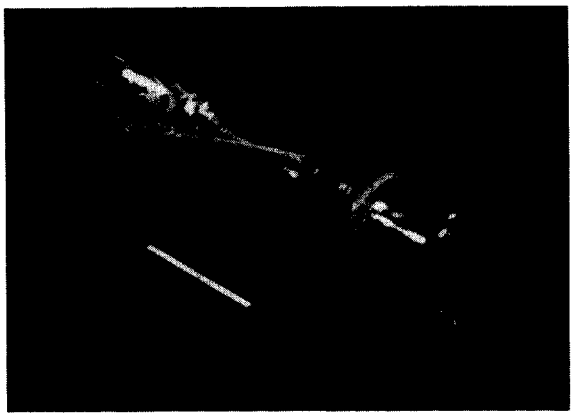

Fig. 1. Photograph of Franck–Hertz tube used in this experiment.

The Leybold version[10] of the Franck–Hertz tube using a concentric electrode system with the indirectly heated cathode in the axis and two grids between cathode and anode proved to be the most suitable for our purposes.

Figure 1 shows a photograph of such a tube. The end of the tube has been replaced by a quartz window. The experimental results will show that the optical quality of the window is of no importance. The tube is custom built by one of the authors at Leybold (S. Pressler). In the meantime a similar tube in a uv-transmitting glass envelope has been developed. This tube is suitable for series production.

The accelerating voltage is measured between cathode and grid 2. A negative bias of about 1.5 V between grid 2 and the anode has little influence on the accelerating potential since this bias causes only negligible distortions of the potential distribution on the cathode side of the fine meshed grid 2. This bias prevents elastically scattered electrons with low energies from reaching the anode.

The cathode is internally connected to one end of the filament, and the accelerating voltage is measured between that filament connection and grid 2.

By means of a temperature-controlled ($\pm$ 1°) oven the mercury vapor pressure in the tube is held constant. The

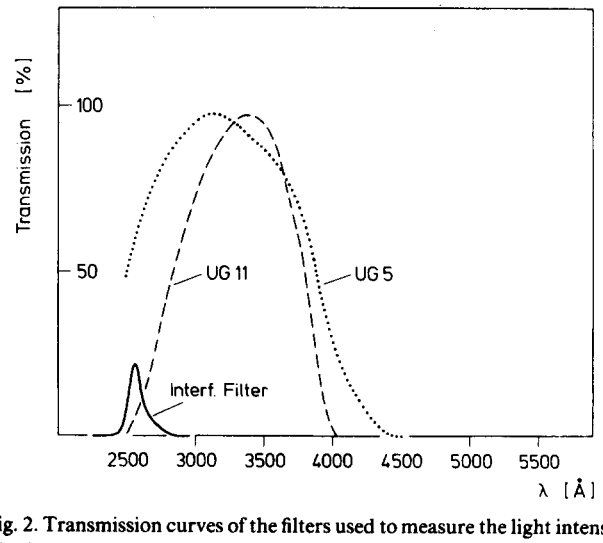

Fig. 2. Transmission curves of the filters used to measure the light intensity. The interference filter is a type G-521-2137 filter with $\lambda_{max} = 2560$ Å; $T_{max} = 22\%$, B.W. = 104 Å manufactured by Oriel Optics.

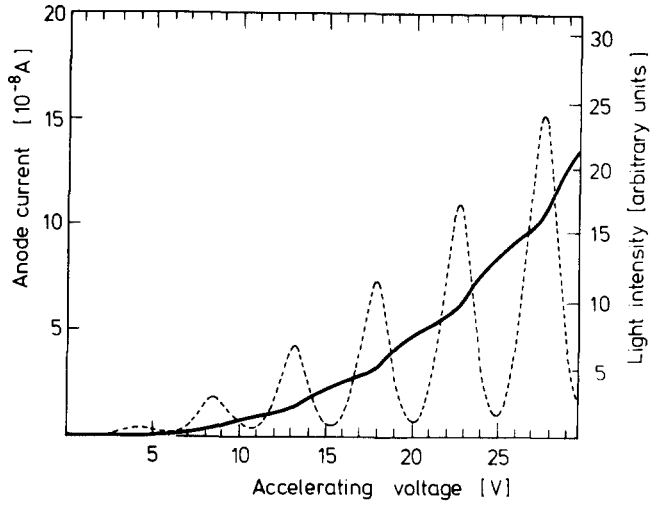

Fig. 3. Anode current and light intensity as a function of accelerating voltage. The dashed curve represents the anode current, the solid curve is the photomultiplier output current representing the light intensity.

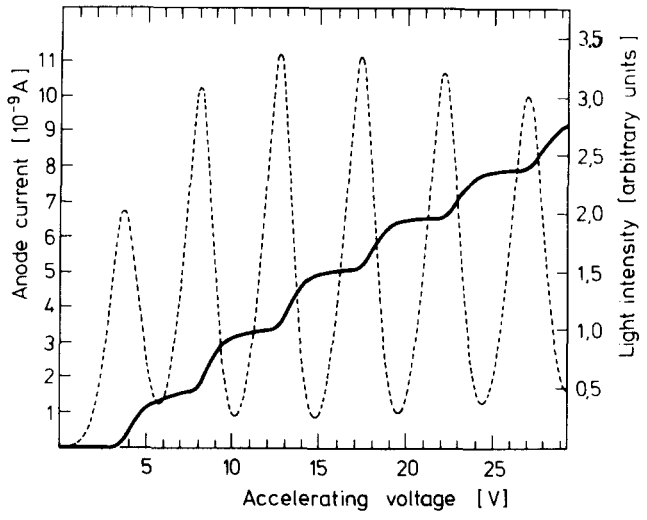

Fig. 5. Current voltage characteristics and light intensity with current stabilization.

light emitted from the volume between grids 1 and 2 can be measured with a photomultiplier[11] through a hole in the rear of the oven.

Excessive noise caused by visible and infrared light from the heated cathode is suppressed by placing a color filter UG5[12] in the path of light between Franck–Hertz tube and photomultiplier. The optical transmission of this filter is shown in Fig. 2.

III. EXPERIMENTAL RESULTS

For small accelerating voltages the anode current characteristics of the Franck–Hertz tube are similar to that of a triode. At an accelerating voltage of about 5 V, however, the anode current reaches a maximum. Here the electrons have for the first time acquired an energy of 4.9 eV. This results in the excitation of mercury atoms by inelastic collisions. The excited state is a $^3P_1$ state, 4.9 eV above the $^1S_0$ ground state. With the spontaneous decay of this state the emission of 2536-Å light should be observed.

Increasing the accelerating voltage further decreases the current as the cross section for inelastic collision[13,14] changes with the electron energy. The current traverses a minimum, when almost every electron has suffered an inelastic collision, and increases again. The light intensity should now remain constant until the electrons can gain another 4.9 eV and the anode current has reached a second maximum. Now the intensity of the 2536-Å emission should increase again.

Figure 3 shows the anode current (dashed curve) and the light intensity (solid curve) versus the accelerating voltage. The decrease in current at integer multiples of the excitation energy can be seen as usual. Instead of the expected stepwise increase in light intensity only small steps superimposed on a steadily increasing function were detected.

However, from a detailed investigation of the operating mode it becomes evident that the conditions to observe a scattering process are rather unfavorable, as the intensity of the primary electron beam varies continuously with the beam energy.

With the current stabilization of Fig. 4 one can, at least for accelerating voltages above 5 V, hold the emission current fairly constant.

The current–voltage characteristic obtained under these

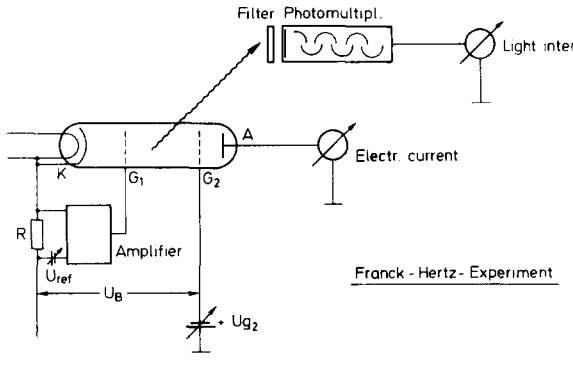

Fig. 4. Reduced schematic. The emission current I of the cathode causes a voltage drop across $R = 100$ K. This current is adjusted by a reference voltage U_{ref}. The voltage difference $IR - U_{ref}$ is fed into an operational amplifier type CA 3140. The internal resistance of the cathode–grid path of the Franck–Hertz tube serves as a feedback resistor. The voltage amplification of the whole circuit is about 40.

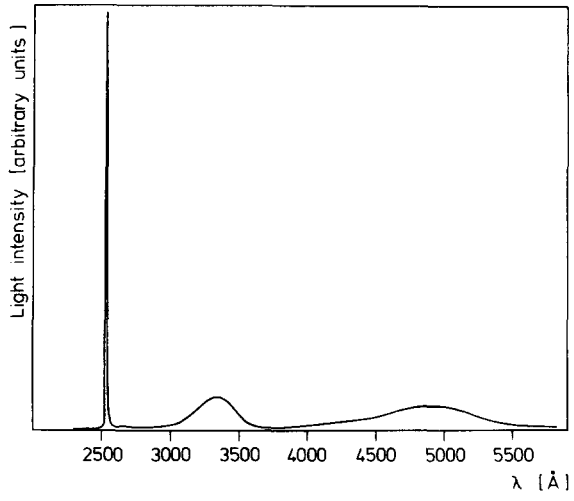

Fig. 6. Spectral emission of mercury vapor at $T = 180$ °C, accelerating voltage 20 V. The second-order spectrum was suppressed by a glass plate in front of the spectrograph at wavelength above 4000 Å.

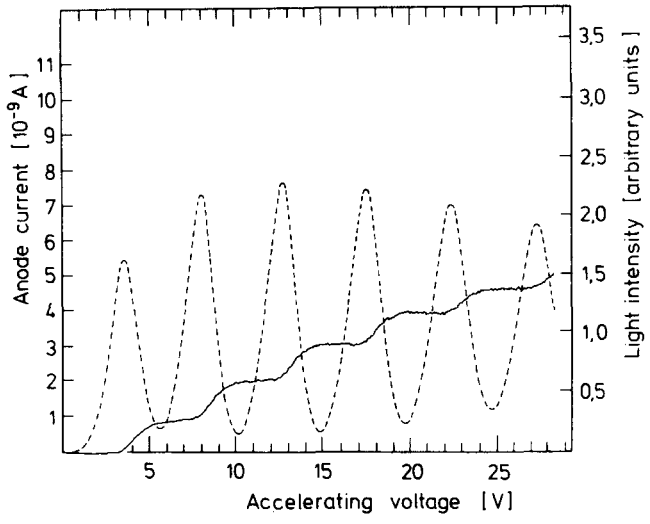

Fig. 7. Franck–Hertz curve and light intensity as a function of accelerating voltage for the 2536-Å line.

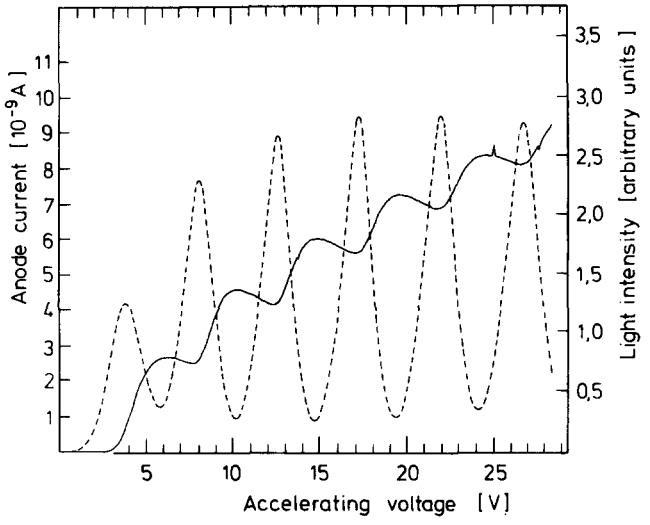

Fig. 8. The 4850-Å continuum.

conditions is shown in Fig. 5, together with the ultraviolet light intensity. The anode current for adjacent maxima does not increase as it does in Fig. 3 and now the stepwise increasing intensity of the ultraviolet emission can be clearly observed.

It is interesting to note that the anode current maxima decrease at higher accelerating voltages as the minimum current and the half-width increases and the maxima become wider. The maximum excitation cross section of the $^3P_1$ state.[13,14] is only about 3×10^{-16} cm^2. At a temperature of 180 °C the vapor pressure is about 10 Torr. As a consequence of this, the probability for elastic scattering with a cross section more than 100 times larger, which eventually will broaden the energy distribution of the electrons is larger than the probability for excitation.

The spectrum of the emitted radiation in Fig. 6 was taken with a grating spectrograph of a focal length of 350 mm, the grating has 1180 lines per mm, blazed at $\lambda = 2500$ Å in first order. For the special range above 3800 Å a grating blazed at 5000 Å was used and a glass plate was inserted between the spectrograph and the Franck–Hertz tube to suppress the second order of the 2536-Å line.

The line appearing at 2536 Å is the mercury resonance of the $^3P_1$–$^1S_0$ transition. This line is accompanied by a broadband between 3000 and 3700 Å centered at 3350 Å, a "continuum"[15,16] arising from the $^3\mathrm{1}_u - X\,^1\Sigma_g^+$ transition of molecular mercury. With the filter used in Fig. 5 the measured intensity included both, the resonance line and the 3350-Å continuum. Thus we have to consider two possible cases for the interpretation of Fig. 5:

(1) The mercury molecule Hg_2 is excited by electron impact and decays into the Hg_2 ground state.

(2) A mercury atom Hg excited by electron impact reacts with a ground-state atom forming an excited molecule which decays into the ground state.

In the first case, the contributions of the resonance line and the continuum have a different origin and are determined not only by different cross sections, but depend also on the ratio of the number density of mercury atoms and molecules. In the second case, the light intensity is uniquely determined by the number density and the cross section of atomic mercury.

The curve of Fig. 7 where only the intensity of 2536-Å line was measured with an interference filter (see Fig. 2) is in favor of case 2.

In a collision between excited and ground-state atoms a dimer molecular state can be formed leading to a transition with a 3350-Å continuum.[13,14] Under these circumstances one can be quite sure that the observed emission is primarily caused by excited mercury atoms.

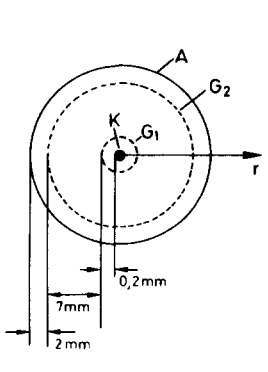

Electrode configuration cross section

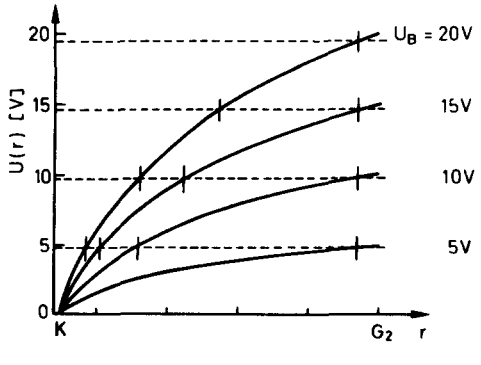

Potential distribution for diff. accelerating voltages

Fig. 9. Cross section through the electrode system and potential distribution for accelerating voltages from 5–20 V between grids 1 and 2. The crosses mark the position of the light emitting annular zones.

The spectrum of Fig. 6 shows another band near 5000 Å. This band arises from a decaying trimer state.[17] The change in light intensity with the accelerating voltage for this band is as one can see from Fig. 8 strongly affected by geometrical factors, whose influence can be roughly explained with the cross section through the electrode system and the potential distribution in Fig. 9. Neglecting the influence of the cylinder ends, the potential changes nearly like the logarithm of the interelectrode distance.

With an accelerating voltage of about 5 V the first annular zone of inelastic scattering originates at grid 2 and with increasing voltage moves toward grid 1. Shortly before the voltage reaches 10 V a second zone starts out from grid 2 and this process is repeated until finally at 20 V four such zones exist between the two grids.

Cathode, grid 1, and grid 2 are held in place by narrow mica bars across the ends of the system. With a decrease in diameter of the light emitting zones the area shaded by the mica bridge increases. The uv light intensity registered by the photomultiplier, however, does not decrease during this process because the uv diffusion at the large vapor pressure in the tube provides a homogeneous illuminated volume. This same argument holds for the light intensity measurement in the 3350-Å band where the diffusion is maintained by the ground-state Hg_2 molecules but not for the 4850-Å band, as the excited trimer decay has no stable ground state.[17] Thus the light intensity curve of Fig. 8 taken with a glass plate as filter displays the influence of the zone structure.

IV. CONCLUSION

With a four electrode tube a complete demonstration of the experiment of Franck and Hertz is possible if the emission current is stabilized. Parallel to the characteristic current maxima the uv light intensity can be measured using a color filter. The light intensity within the transmission range of this filter is proportional to the number of mercury atoms in the $^3P_1$ state for the 2536-Å line as well as for the 3350-Å band. Therefore it is not necessary to use an expensive narrow interference filter with relatively low transmission resulting in increased multiplier noise.

The steps in the light intensity curve require the same interpretation as the current maxima of the Franck–Hertz curve. Light emission after excitation and discrete energy loss of exciting electrons form a direct experimental check of the Bohr theory of atoms.

ACKNOWLEDGMENTS

We are glad to thank U. Hauser for initiating this work. The help of E. Krämer is gratefully acknowledged. We are indebted to W. Neuwirth, R. Schieder, and K. Bielke for many helpful discussions and to G. Winnewisser and T. Pauls for reading the manuscript. We also thank Th. Becker for the drawings and the reproductions.

[1]J. Franck and G. Hertz, Verh. Dtsch. Phys. Ges. **16**, 457 (1914).
[2]J. Franck and G. Hertz, Verh. Dtsch. Phys. Ges. **16**, 512 (1914).
[3]See, e.g., J. Franck and E. Einsporn, Z. Phys. **2**, 18 (1920); E. Einsporn, Z. Phys. **5**, 208 (1921); J. Franck, Z. Phys. Chem. Unterr. **41**, 18 (1928); J. Franck and P. Jordan, *Anregung von Quantensprüngen durch Stoss* (Springer-Verlag, Berlin, 1926); P.D. Foote, W. F. Meggers, and F. L. Mohler, Astrophys. J. **55**, 145 (1922).
[4]Bernheim, Gossard, and Pound, Am. J. Phys. **24**, 630 (1956).
[5]J. W. Dewdney, Am. J. Phys. **27**, 645 (1959).
[6]R. E. Adelberger and K. F. Kinsey, Am. J. Phys. **40**, 349 (1972).
[7]R. J. Genolio, Am. J. Phys. **41**, 288 (1973).
[8]M. Füssenich, H. Jodl, and G. Theysohn, Phys. Didakt. **1**, 15 (1980).
[9]Neva, Dr. Vatter KG, Geislingen, Germany.
[10]Leybold–Heraeus, Cologne, Germany.
[11]Side window tube with Corning 9741 glass envelope (transmission to 2000 Å), type 9781B, manufactured by EMI.
[12]UG5, 1 mm thick from Schott Gen., Jenaer Glaswerke, Mainz, Germany.
[13]H. S. W. Massey, H. H. S. Burhop, and H. G. Gilbody, *Electronic and Ionic Impact Phenomena Vol. I* (Clarendon, Oxford, 1969).
[14]H. S. W. Massey, in *Handbuch der Physik*, edited by S. Flügge (Springer-Verlag, Heidelberg, 1956), p. 328.
[15]Tables of constants and numerical data, *foundet by Ch. Marie (1909)* (Pergamon, New York, 1970), p. 203.
[16]A. C. G. Mitchell and M. W. Zemansky, *Resonance Radiation and Excited Atoms* (Cambridge University, Cambridge, 1961), p. 89.
[17]M. Stock, E. W. Smith, R. F. Drullinger, M. M. Hessel, and J. Pourcin, J. Chem. Phys. **68**, 1785 (1978).